CellPress

Current Biology

Review

Dynamic changes in epithelial cell packing during tissue morphogenesis

Sandra B. Lemke[1] and Celeste M. Nelson[1,2,*]
[1]Department of Chemical and Biological Engineering, Princeton University, Princeton, NJ 08544, USA
[2]Department of Molecular Biology, Princeton University, Princeton, NJ 08544, USA
*Correspondence: celesten@princeton.edu
https://doi.org/10.1016/j.cub.2021.07.078

SUMMARY

Cell packing — the spatial arrangement of cells — determines the shapes of organs. Recently, investigations of organ development in a variety of model organisms have uncovered cellular mechanisms that are used by epithelial tissues to change cell packing, and thereby their shapes, to generate functional architectures. Here, we review these cellular mechanisms across a wide variety of developmental processes in vertebrates and invertebrates and identify a set of common motifs in the morphogenesis toolbox that, in combination, appear to allow any change in tissue shape. We focus on tissue elongation, folding and invagination, and branching. We also highlight how these morphogenetic processes are achieved by cell-shape changes, cell rearrangements, and oriented cell division. Finally, we describe approaches that have the potential to engineer three-dimensional tissues for both basic science and translational purposes. This review provides a framework for future analyses of how tissues are shaped by the dynamics of epithelial cell packing.

Introduction

Tissues are collections of cells, and the structure of a tissue is intimately linked to its function. For example, lung alveoli and the pulmonary vasculature must be in close proximity throughout the lung for efficient oxygen exchange[1]. Similarly, the kidney ducts and the renal vasculature must be adjacent to each other in order to remove waste products and excess fluid from the body[2]. Packing of cells in a tissue is defined by the spatial organization of their neighbors and, in turn, packing defines juxtacrine (and paracrine) interactions, placement of resident stem/progenitor cells, and the composition of the stem cell niche[3]. Cell–cell adhesion allows coordination and mechanical propagation of information that instructs collective cell behaviors. Thus, the function of a tissue is more than the sum of its constituent cells.

Epithelial cells typically form sheets that line organs and thereby create barriers between compartments. Changes in cell shape and cell rearrangements result in dynamic changes in epithelial cell packing that drive changes in tissue shape and promote the formation of functional, three-dimensional (3D) organs. Vice versa, changes in tissue shape, such as tissue stretching or folding, result in changes in cell packing and cell shape. Here, we review recent work studying the packing of epithelial cells and highlight how these cells shape tissues during morphogenesis. We focus on morphogenetic processes in which epithelial tissues elongate, fold and invaginate, or branch and we identify common motifs used by the cells to achieve these changes in tissue shape. Recent advances in time-lapse and quantitative imaging analysis have enabled the quantitative characterization of a number of morphogenetic processes, including elongation of the *Drosophila* wing epithelium[4,5]. When combined with computational modeling, these approaches now permit the quantification of the relative contributions of cell-shape changes, rearrangements, and oriented cell divisions to the overall change in tissue shape.

Cell shape and packing in 3D epithelial tissues

Epithelial cells have the remarkable ability to adopt a variety of shapes depending on their position within a tissue, and this has consequences for their function (Figure 1A). Large and flat cells are called squamous, based on the Latin word *squama* meaning scale. Cells that are similar in height and width are called cuboidal, and cells that are taller than they are wide are called columnar. While many epithelia exist as monolayers, epithelial cells can also form multilayered stratified tissues. Pseudostratified epithelia consist of a single layer of cells that achieve dense packing by shifting their cell bodies and nuclei apically or basally relative to their neighbors.

Cell shape and function are intimately linked

The epithelial cell shape that is found in a given organ depends on the function of the tissue. For example, thin cell layers allow rapid diffusion, so squamous epithelia are present in lung alveoli to enable gas exchange. Cuboidal epithelia are often found in ducts of glands like the kidney, where they perform functions related to absorption and secretion. Columnar epithelia that are present in the gut are responsible for taking up nutrients and transporting them across the gut lining. Since this process relies on active transport rather than diffusion, the larger distances provided by a columnar geometry can be overcome. Furthermore, the increased thickness of columnar epithelia compared with squamous and cuboidal epithelia means that they are less fragile and provide a mechanically stable barrier. Pseudostratified epithelia are found, for example, in the lung trachea and bronchi. Close packing of different epithelial cell types localizes cells to positions appropriate for their functions: goblet cells secrete mucus to protect the airway epithelium, and ciliated

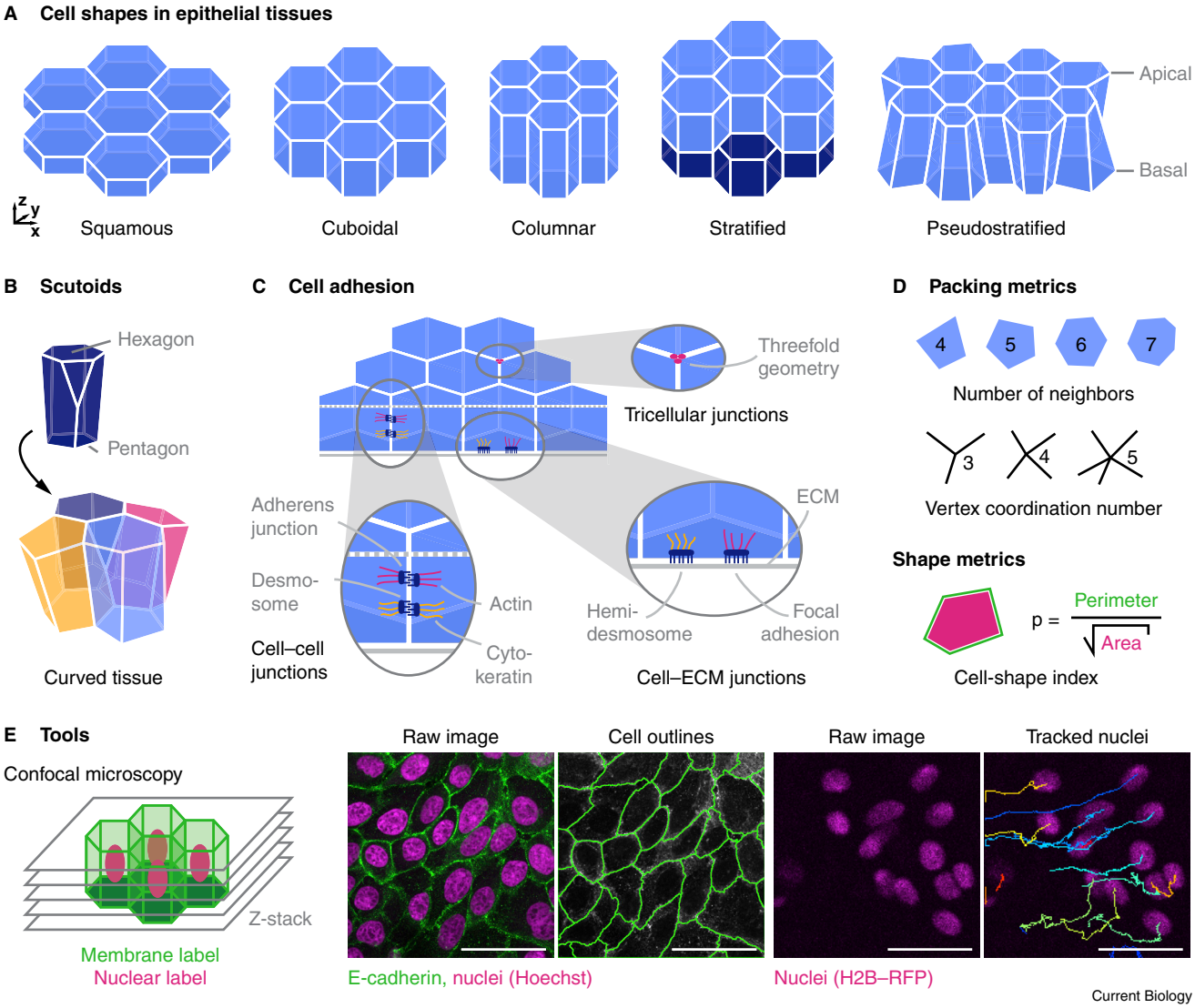

Figure 1. Epithelial cell shapes and interactions.
(A) Schematics illustrating typical cell shapes observed in epithelial tissues. (B) Schematic illustrating the scutoid, a recently discovered cell shape that is found predominantly in curved tissues. Note that the cell has different neighbors in its apical and basal planes. (C) Schematic illustrating cell–cell and cell–ECM adhesions. Cell–cell interactions can have either a twofold symmetry at cell faces or a threefold symmetry at tricellular junctions. (D) Metrics used to describe the packing and shape of epithelial cells. (E) Tools for experimentally detecting and quantifying epithelial cell shapes: confocal microscopy can be used to acquire images of cells either expressing fluorescent markers or stained with antibodies. Images of a membrane label such as E-cadherin can be used to automatically detect cell outlines. The outlines shown here were created using the ImageJ Plugin Tissue Analyzer[25]. A fluorescent protein such as H2B–RFP can be used to track cell movements. Tracks shown here were created using the ImageJ Plugin TrackMate[26] from a 10-hour-long time-lapse video of MCF10A mammary epithelial cells. Scale bars are 50 μm. Microscopy images in (E) courtesy of Payam Farahani.

cells move mucus and trapped particles out of the lung. Together, these two cell types protect the more distal airways in the lung from inhaled particulates.

The cell shapes described above are all essentially prisms with polygonal apical and basal surfaces (illustrated as hexagons for simplicity in Figure 1A). However, a new scutoid cell shape was identified recently that is often found in curved epithelial tissues, such as in the salivary gland[6]. As opposed to prism-shaped cells, scutoids do not form contacts with the same neighbors at their apical and basal planes. The scutoid is best described as a pentagon and a hexagon connected to each other such that one corner appears to have been sliced off on one side (Figure 1B). Aside from enabling the efficient packing of epithelial cells into curved tissues, scutoids can be viewed as a transitional state in which a cell has exchanged neighbors on either its apical or basal surface but not both. Scutoids have therefore been predicted to allow dynamic rearrangements of cells within 3D tissues.

Heterogeneous cell sizes within an epithelium can also lead to cell rearrangements and thereby affect cell packing. Abnormally small cells, like many cancer cells, tend to disperse within a tissue. Mathematical modeling in combination with microscopy

analysis of clones containing small cells in the *Drosophila* wing disc epithelium has revealed that a tissue reaches an energetically favorable state when small cells reduce their number of neighbors by dispersing between normally sized cells[7]. Thus, heterogeneities in cell size can drive cell rearrangements while keeping the strength of cell–cell adhesion constant based solely on geometrical constraints.

Cell adhesions shape and hold epithelial tissues together

Cell–cell junctions and cell–extracellular matrix (ECM) junctions hold epithelial tissues together (Figure 1C). These junctions can be grouped according to whether they connect to cytokeratin-containing intermediate filaments or to the actin cytoskeleton. Cytokeratins bind to desmosomes at cell–cell contacts and hemidesmosomes at cell–ECM contacts. Together, these junctions and the cytokeratin network ensure tissue integrity and provide tissue elasticity, allowing epithelia to bend and stretch. Actin filaments bind to adherens junctions, which connect cells to each other via cadherins, and to focal adhesions, which connect cells to the ECM via integrins. Since the actomyosin network is contractile, these junctions together with the actin cytoskeleton can change the shape of an epithelium to create folds and invaginations.

Vertebrate cells also form tight junctions, which seal the gap between neighbors and create a barrier to water and solutes. This barrier function is especially important for epithelial tissues like those in the gut, the kidney, or the mammary gland. Tight connections between neighboring cells leave one potential weak spot at the point where three cells meet. To create a tight barrier, these tricellular junctions require a special structure with a threefold geometry[8,9]. Recent work in invertebrates revealed that tricellular junctions can transiently open and close to allow for controlled transport of components, such as yolk, between epithelial cells[10]. To permit cell rearrangements while maintaining tissue integrity, the strength of adhesion at tricellular junctions is dynamically regulated in a force-dependent manner[11]. Aberrantly increased adhesion results in the arrest of the cell rearrangements required for tissue elongation. Furthermore, tricellular junctions play active roles during morphogenesis as sensors of cell shape that help to orient cell division[12].

Cell shape and adhesion thus act together to give an epithelial tissue its morphology, durability, flexibility, and barrier function. The shapes and packing of epithelial cells have therefore been studied extensively in a variety of model tissues. In the next paragraphs, we review common metrics that are used to describe epithelial cell shape and packing, and we highlight microscopy and software tools that are used to visualize epithelial packing.

Metrics used to characterize cell packing

The simplest metric to describe epithelial cell packing is to characterize each cell by the number of its neighbors in two dimensions (2D) (Figure 1D). Similarly, each vertex in an epithelial cell sheet can be characterized by the number of cells that meet at this point. To characterize the 3D shape of an epithelial tissue, local curvature of epithelial cell sheets can be quantified. Furthermore, to simplify the analysis of cell packing in 3D, curved tissues can be projected onto a 2D surface[13] to take advantage of 2D metrics for the analysis of cell shape and packing[14].

As a first approximation, the shapes and packing of cells in a tissue can be described using the same physical concepts as those for soap bubbles in a foam, an idea that was described in seminal work by D'Arcy Thompson[15]. However, cells are not passive objects like soap bubbles and can actively change their shapes: cells can contract, move, and squeeze past each other and dynamically regulate the strength of adhesions to their neighbors and to the ECM[16,17]. One metric that can capture these active and dynamic changes in cell shape is the cell-shape index (Figure 1D), which is calculated as the perimeter of a cell divided by the square root of its area. For a given area, the shape index is smallest for a circular cell and increases for more elongated cells. Thus, cells that establish short contacts with their neighbors have a small shape index, which is typically associated with a solid-like or 'jammed' tissue containing cells that do not frequently exchange their neighbors. Conversely, cells that establish longer intercellular contacts have a larger shape index, which is typically associated with a more fluid-like or 'unjammed' tissue containing cells that readily exchange neighbors[18]. The cell-shape index is a useful metric to analyze shape in the context of tissue fluidity. For example, germband extension in *Drosophila* is associated with an increase in both cell-shape index and cell movements within the tissue[19]. A large cell-shape index alone, however, is not sufficient to conclude that cells readily rearrange because external forces on a tissue can deform cells in the absence of rearrangements[20]. A cell-shape index analysis should therefore be combined with time-lapse imaging techniques to make conclusions about tissue fluidity.

Microscopy and image-analysis tools for characterizing epithelial tissues

The visualization and quantification of cell packing during morphogenesis requires techniques that are suitable for acquiring 3D images, like scanning confocal, spinning disc, two-photon, or light-sheet microscopy (Figure 1E). The geometry of cells holds a plethora of information and force-inference methods can even provide insight into mechanical forces and pressures in a non-invasive manner from static images[21–24]. Quantification of cell shape at different time points during morphogenesis is enabled by fluorescent membrane makers, such as membrane-bound GFP for live imaging, or immunofluorescence analysis of E-cadherin for fixed samples. A nuclear marker such as H2B–GFP can be used instead of or in addition to the membrane marker to track cells during time-lapse analysis.

Several software tools have been recently released to enable automated outlining and tracking of cells. Tissue Analyzer (previously called Packing Analyzer) is an ImageJ plugin that automatically detects cell borders using an interactive interface that allows the user to adjust parameters for automatic segmentation and to manually correct cell outlines[25]. IMARIS has emerged as a powerful commercially available platform for handling 3D datasets and comes with a suite of tools for 3D visualization, feature detection, and tracking. An open-source alternative for cell tracking that is also capable of dealing with 3D data is the ImageJ plugin TrackMate[26]. TrackMate provides feature detection and tracking in 3D and the tracking results can be exported as text files or visualized as overlays on image stacks in ImageJ. Examples of automated cell outlining using Tissue Analyzer and cell tracking using TrackMate are shown in Figure 1E.

An alternative open-source platform is CellProfiler[27], which is a Python package with a graphical user interface that allows the creation of image-analysis pipelines. The user can either create their own scripts or take advantage of analysis pipelines created by others that are readily shared in the community. Starting with the third CellProfiler release, the software can also handle 3D data like the platforms discussed above.

Morphogenetic processes driven by dynamic changes in epithelial cell packing

Morphogenetic processes create complex shapes to form a variety of organs. Here, we group morphogenetic processes according to the change in tissue shape that is generated and analyze the motifs that are used to accomplish this change. We begin by describing motifs used during tissue expansion and elongation, fairly simple changes in tissue shape, and then proceed to discuss more complex shape changes, such as invagination and branching. We emphasize that any change in tissue shape, regardless of its complexity, can be achieved by combining simple motifs, such as cell-shape changes, cell rearrangements, and oriented cell divisions. This concept has been explored quantitatively in recent years, facilitated by analytical tools created to describe changes in tissue shape fully from cellular dynamics[4,28,29].

Tissue expansion and elongation

In many developmental events, such as limb morphogenesis, tissues expand and elongate. Tissue expansion can be achieved by changes in cell shape, for example from cuboidal to squamous, and by cell division. Tissues can elongate in a specific direction by changes in cell shape, cell rearrangements, or oriented cell divisions (Figure 2A). All three strategies can be driven by cell-intrinsic behaviors or by external forces exerted on the tissue. For a detailed description of the molecular mechanisms regulating cytoskeletal force and adhesion to orchestrate tissue-shape changes in morphogenesis, we refer the reader to an excellent recent review by Clarke and Martin[30]. In principle, a single cellular strategy would suffice to elongate a tissue; however, these strategies are often connected, especially in vertebrate systems. For example, elongated cells preferentially divide along their long axis. As a consequence, cell elongation and oriented cell division can work together to promote tissue elongation. That said, the bias of cell division according to cell shape can be overridden by the presence of tension across a tissue, for example the *Drosophila* germband[31] or the follicle epithelium[32], or by tension on a multicellular actin cable at segment boundaries[33].

Tissue elongation can also be achieved purely by cell rearrangements, such as through shrinkage and growth of new cell boundaries (T1 transitions) or rosette formation and resolution (Figure 2B). As a result, cells change neighbors and the tissue elongates in the direction of T1 or rosette resolution. Conversely, tissue narrowing can be achieved by rearrangements in the opposite direction or by extrusion of cells apically or basally[34,35]. How easily cells can exchange neighbors affects tissue fluidity. Tissues with few neighbor exchanges resulting in a solid-like state have been described as jammed, whereas those with dynamic rearrangements resulting in a fluid-like state have been described as unjammed[18,36,37].

Expansion of the serosa epithelium around the insect embryo

The concept of tissues behaving as solids or fluids has recently been applied to an epithelial sheet called the serosa, which expands and wraps around the embryo of insects like the flour beetle *Tribolium castaneum* during gastrulation[38]. The serosa first caps the anterior dorsal side of the embryo and then expands around the entire ellipsoidal embryo and seals it on the ventral side (Figure 2C). To achieve expansion in the absence of cell division, the cells increase their surface area under mechanical tension. Expansion is accompanied by local compaction at the leading edge of the epithelium after it passes the equator of the embryo and closes the gap on the ventral side. During this process, cells on the dorsal side show hexagonal packing, isotropic stretching, and rare neighbor exchanges indicative of a solid-like or jammed tissue state. Simultaneously, cells on the ventral side around the constricting leading edge show irregular packing and frequent neighbor exchanges, indicative of a fluid-like or unjammed state. The fluidization allows cells to move away from the leading edge and integrate into the tissue, thereby shrinking the circumference of the gap. Together, local solid-like (jammed) and fluid-like (unjammed) tissue behaviors allow the serosal epithelium to acquire the 3D ellipsoidal shape required to encompass the embryo. The concept of jamming has also recently been applied to other developing tissues, for example during elongation of the vertebrate body axis[39,40]. Here, fluid-like behavior is observed at the extending, posterior end of the zebrafish midline, whereas the more anterior end exhibits solid-like behavior: the tissue thus elongates along the body axis.

Elongation of the Drosophila *wing epithelium*

The *Drosophila* wing is another example of an elongated tissue. The cellular strategies that contribute to tissue elongation during wing development have been described quantitatively in recent years by combining long-term time-lapse imaging with new computational approaches (reviewed in Diaz-de-la-Loza and Thompson[5]). The wing of the adult fly forms from the wing imaginal disc, which grows extensively during larval development. The pouch area, which forms the wing blade during later stages of development, grows anisotropically at this stage, elongating dorsoventrally (Figure 2D). Quantitative analysis of cellular contributions revealed that tissue elongation is achieved by cell elongation, cell rearrangements through T1 transitions, and oriented cell divisions, each with similar contributions to the overall change in tissue shape[41].

The wing imaginal disc then everts by folding along the dorsoventral border of the wing pouch and bulging out to form an epithelial pouch during pupal development (Figure 2D). Elongation of the wing at this stage is achieved by a columnar-to-cuboidal cell-shape change that reduces cell height and increases cell width, driving surface extension[42]. To achieve an oval rather than a round shape, cell expansion is accompanied by convergent-extension movements that narrow and lengthen the tissue in the proximal–distal direction.

At this stage, the cells that will form the hinge area of the wing and the cells that will form the wing blade occupy roughly equal areas of the wing tissue. The wing blade tissue next elongates along its proximal–distal axis (Figure 2D). Elongation results from contraction of the hinge tissue, which pulls on the blade

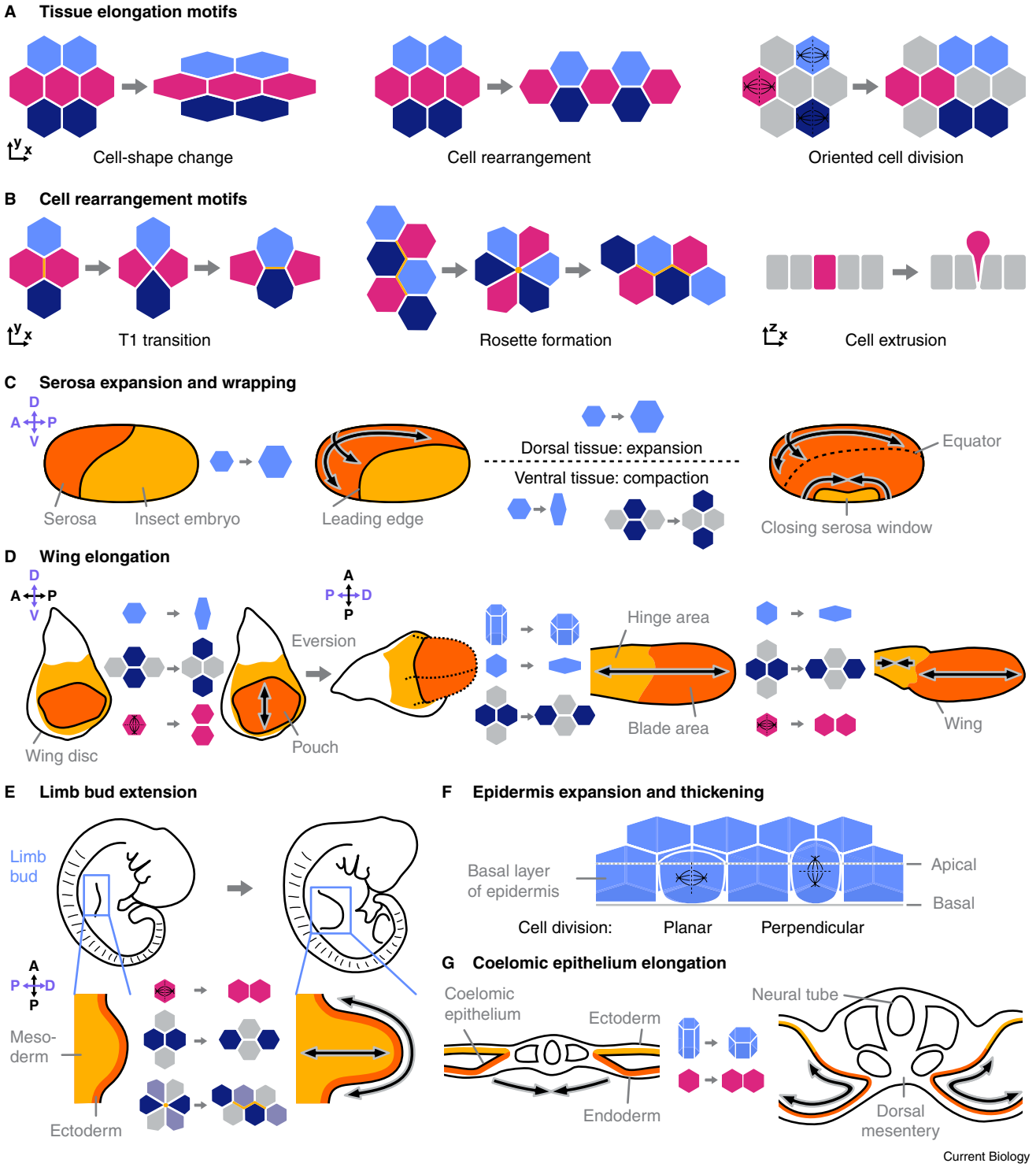

Figure 2. Mechanisms used to achieve elongation of epithelial tissues.
(A) Schematics illustrating motifs that drive tissue elongation. Note that tissue elongation may result from a combination of these motifs. (B) Schematics illustrating mechanisms of cell rearrangement. Shortening and elongating cell boundaries are highlighted in orange. (C–G) Schematics illustrating morphogenetic processes that require tissue expansion and elongation. Icons of the cellular motifs introduced above indicate how tissue elongation is achieved at the respective developmental steps (light blue, cell-shape change; dark blue, cell rearrangement; magenta, oriented cell division). A-P, anterior–posterior; D-V, dorsal–ventral; P-D, proximal–distal. (C) Serosa expansion and wrapping. The serosal epithelium of the red flour beetle expands around the ellipsoidal embryo and seals it on the ventral side. While the tissue on the dorsal side expands, the tissue on the ventral side compacts to close the serosa window. (D) Wing elongation. The *Drosophila* wing forms from the wing imaginal disc. The pouch area of the disc elongates dorsoventrally and then everts, folding in on itself. Next the wing elongates

(legend continued on next page)

tissue that is anchored to the overlying chitinous cuticle[43,44]. Due to this anchorage, tension builds up in the blade tissue, resulting in cell elongation and cell rearrangements through T1 transitions[44,45]. Oriented cell divisions also contribute to tissue elongation, albeit to a lesser extent. In contrast to the cell elongation and T1 transitions, cell divisions are thought to be oriented independently from the external tension on the tissue since the preferred angle of division persists even if tension is released[44]. Nevertheless, the overall tissue shape strongly depends on tension built up across the wing blade. If anchorage to the cuticle is disrupted by genetic perturbations or laser ablation, the wing predictably becomes less elongated in areas where anchorage is missing[43,44]. The *Drosophila* wing is therefore shaped by a series of tissue-elongation steps that are achieved by a combination of cell-shape changes, cell rearrangements, and oriented cell division.

Limb bud elongation in vertebrates

Like the *Drosophila* wing, the vertebrate limb also forms by proximal–distal elongation of a tissue referred to as the limb bud (Figure 2E). The limb bud consists of a mesodermal core covered by an ectodermal epithelium. The bud is formed by directional movement of the mesoderm, which pushes into the ectoderm and thereby creates an outward bulge[46]. The conventional view was that a gradient of isotropic mesodermal cell proliferation is sufficient to explain the elongation of the limb bud. However, quantification of cell proliferation rates and local tissue deformation in combination with mathematical modeling revealed that directional tissue deformation, not local growth, is the main driver of limb elongation[47–49].

The ectodermal epithelium lining the limb bud needs to bulge out and expand to accommodate the elongating mesodermal core (Figure 2E). The ectoderm experiences tension in the proximal–distal orientation because of the elongation of the mesoderm and cell intercalation at the distal end of the bud called the apical ectodermal ridge (AER)[50]. This tension favors rosette resolution along the proximal–distal axis, thereby leading to tissue expansion. Furthermore, time-lapse imaging of the mouse limb bud revealed that tissue expansion is also driven by cell division followed immediately by separation of the daughter cells. Rather than staying as neighbors, the daughter cells separate as they reintegrate into the epithelial sheet, similar to a T1 transition, leading to additional elongation of the tissue by one cell diameter. Thus, the vertebrate limb bud elongates because of cell rearrangements that are biased to resolve in the proximal–distal direction due to tissue-level tension.

Expansion and thickening of the epidermis

Similar to the epithelium lining the limb bud, the entire skin of the mouse embryo must expand as the embryo grows. Cell division in the epidermal layer of the skin can occur either within or perpendicular to the plane of the epidermis (Figure 2F). While in-plane cell divisions lead to expansion of the skin, perpendicular divisions lead to thickening of the skin layers. If the skin is stretched by the growing embryo, cells elongate and divide in the direction of tension to reduce stress on the tissue[51]. Therefore, skin expansion and thickening can be balanced by epidermal cells using their geometry as a readout, independent of any planar cell polarity cues.

Shaping of the body cavity in vertebrates

Time-lapse imaging is a valuable tool for studying changes in epithelial cell packing that drive morphogenesis. However, processes that are not accessible to live imaging can also be analyzed and understood by careful measurements of cell packing in fixed samples that provide snapshots of morphogenesis. For example, this approach has been used to characterize elongation of the coelomic epithelia that line the body cavity (coelom) in chicken embryos[52]. During development, the coelomic epithelia on either side of the embryo elongate to meet at the embryonic midline and form the dorsal mesentery that acts as an anchor for the gut tube in the abdomen (Figure 2G). Measurements of the thickness of the pseudostratified epithelia revealed that the cells flatten by about 25% as new cells are added to the tissue. Assuming that the cells maintain a constant volume, these two observations can explain elongation of the coelomic epithelium.

Tissue folding and invagination

Generation of folds and invaginations is a common motif found in morphogenesis. Invaginations typically occur during the formation of internal structures such as glands, and folds are often used to increase surface area, for example in the gut. Many of these structures are either formed by apical constriction of the cells in the center of the future fold or by buckling of a tissue experiencing compressive forces (Figure 3A). Recently, extrusion of apoptotic cells and the associated apical–basal forces have also been shown to contribute to tissue folding during morphogenesis of the *Drosophila* leg[53].

Coordinated ventral invagination and dorsal expansion during Drosophila *gastrulation*

Apical constriction during *Drosophila* gastrulation leads to invagination of the mesoderm, which has been studied in detail over the past few decades[54–56]. Much of the work focusing on the constricting cells themselves has been reviewed elsewhere[30,57]. Here, we review work focusing on the embryonic tissue as a whole to analyze how neighboring tissues contribute to invagination. As central cells at the ventral midline constrict apically, peripheral mesoderm cells stretch to accommodate the constriction, while neighboring lateral cells do not stretch (Figure 3B). F-actin density in peripheral mesoderm cells is significantly lower than in neighboring lateral cells; therefore, the lower F-actin density is thought to allow the peripheral mesoderm cells to stretch[58]. Thus, apical constriction and cell stretching in neighboring cells work together to form the ventral furrow during *Drosophila* gastrulation.

Whole-embryo light-sheet imaging revealed that constriction and stretching of mesodermal cells are not sufficient for furrow

proximodistally. Compaction of the hinge area leads to further elongation of the blade area. (E) Limb bud extension. The mouse limb bud extends as the mesoderm grows and moves into the limb bud. The mesoderm, together with cell intercalations in the endoderm at the tip of the bud (the apical ectodermal ridge), creates tension across the ectodermal epithelium proximodistally, resulting in oriented cell divisions and cell rearrangements that contribute to the elongation of the limb bud. (F) Epidermis expansion and thickening. Planar cell divisions in the basal layer of the epidermis contribute to expansion, and perpendicular cell divisions contribute to thickening of the skin layers. (G) Coelomic epithelium elongation. In dorsoventral cross-sections of chicken embryos, flattening of the coelomic epithelium lining the body cavity of the embryo can be observed. Flattening, together with the addition of cells, allows the coelomic epithelia to meet at the ventral midline and form the dorsal mesentery that anchors the gut tube.

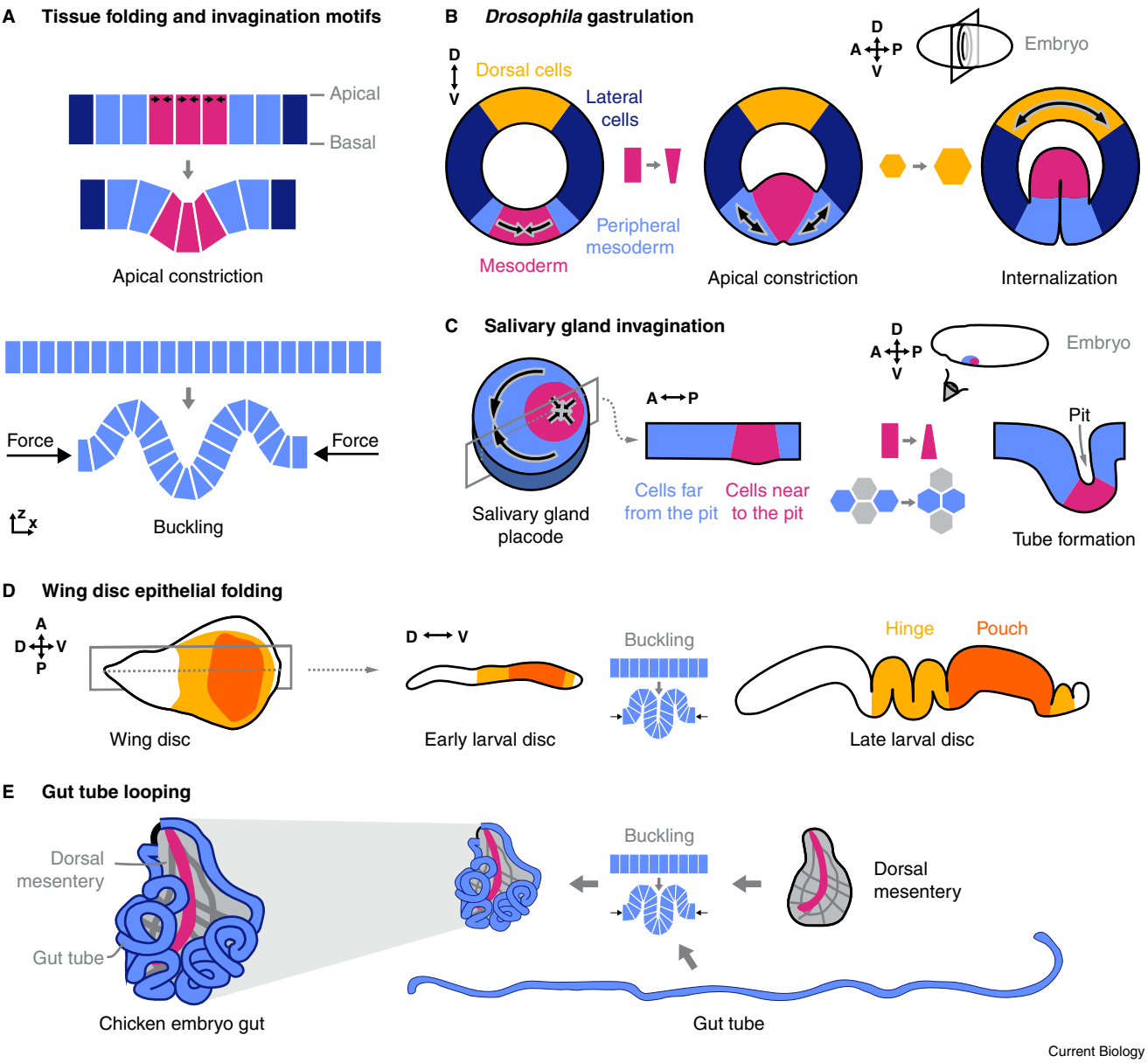

Figure 3. Mechanisms used to achieve folding and invagination of epithelial tissues.
(A) Schematic illustrating developmental motifs that result in tissue folding and invagination. (B–E) Examples of morphogenetic processes requiring folding and invagination to form organs. Icons of the cellular motifs introduced in Figures 2A and 3A indicate how tissue folding and invagination are achieved at the respective developmental steps. A-P, anterior–posterior; D-V, dorsal–ventral. (B) *Drosophila* gastrulation. Mesodermal cells constrict apically to form the ventral furrow; the furrow then invaginates as the dorsal cells expand while lateral cells stay compact. (C) Salivary gland invagination. The *Drosophila* salivary gland invaginates from the salivary placode on the ventral side of the embryo. Cells near the future invagination site (pit) constrict apically. To allow these cells to invaginate, the cells further from the pit intercalate circumferentially, leading to radial tissue elongation towards the pit and formation of a tube. (D) *Drosophila* wing disc epithelial folding. Heterogeneous growth and thickening of the wing disc in a defined pattern lead to buckling of the epithelium in a reproducible manner to form hinge and pouch regions. (E) Gut tube looping in the chicken embryo. Differences in growth rates of the dorsal mesentery and the gut tube lead to buckling and formation of stereotyped loops. For comparison, the gut tube and the mesentery are shown to scale in their dissected, relaxed states.

invagination[59]. To allow invagination, the tissues on the lateral sides of the embryo need to move towards the furrow and the tissue on the dorsal side of the embryo needs to stretch (Figure 3B). If this movement of lateral tissues is blocked by cauterizing the tissue to the eggshell, the ventral cells still constrict apically but can no longer invaginate. To allow expansion, the dorsal tissue softens by reducing actomyosin levels, while the lateral tissue remains stiff[59]. In fact, quantification of the amount of actomyosin, which controls tissue stiffness, allows one to predict the flow patterns of cells during gastrulation using a viscous model[60]. Thus, invagination of the ventral furrow during *Drosophila* gastrulation is driven by apical constriction of the mesoderm in concert with tissue stretching and changes in flow patterns throughout the embryo.

Apical constriction and cell rearrangements during tube formation of the salivary gland

Similarly, apical constriction in a circular area can initiate the formation of tubes from flat, epithelial sheets. This process has been characterized in detail by time-lapse imaging and cell tracking using the *Drosophila* salivary gland as a model system[13,61]. The salivary gland invaginates from approximately 100 cells of the ventral epithelium lining the embryo — the salivary gland placode (Figure 3C). Cells near the pit, which forms as the tissue invaginates, constrict apically such that the cells become wedge shaped[13]. This constriction results in tension on the cells further from the pit, which favors the resolution of T1 transitions towards the pit and thereby leads to radial elongation of the tissue. Thus, the tube forms by a combination of apical constriction and elongation of the neighboring tissue by cell intercalation.

Buckling morphogenesis of the Drosophila *wing disc*

In addition to apical constriction, buckling morphogenesis is a common motif used to create tissue folds[62]. Compressive forces acting in-plane on an epithelium result in out-of-plane buckling to relieve stress on the tissue (Figure 3A). The shape and positioning of the buckles or folds are dictated by the material properties of the tissue, such as its elastic modulus and thickness. Compressive forces can be generated either by contraction of a neighboring tissue or by faster growth of a tissue compared with neighboring structures.

The *Drosophila* wing disc epithelium buckles during larval development and the positioning of the folds is highly stereotyped and important for morphogenesis. Tozluoglu *et al.*[63] investigated the minimum set of requirements for initiating folds in the correct position by quantifying local growth rates and by performing computational modeling. Their study revealed that spatial and temporal heterogeneity of growth is key in determining the positioning of folds independent of active forces like apical constriction. High growth rates and thickening of the columnar epithelium in the pouch area of the disc lead to the formation of folds at the borders of this area (Figure 3D). The underlying basement membrane, which confines the wing disc, contributes to shaping and maintenance of the epithelial folds[63–65]. Thus, compressive forces generated by heterogeneous growth in a confined tissue like the wing disc lead to reproducible patterns of buckling.

Buckling morphogenesis of the vertebrate gut

Another tissue that is shaped by buckling morphogenesis is the gut. Efficient absorption of nutrients requires a large surface area within a confined volume. This requirement is achieved on two levels: buckling of the epithelium lining the gut tube; and buckling of the tube inside the abdomen[66]. The human abdomen can thereby accommodate a 5-meter-long tube with a surface area of about 32 m^2 (equivalent to about half a badminton court)[67].

The gut tube is surrounded by smooth muscle layers. Studies using the chicken embryonic gut as a model system revealed that these smooth muscle layers restrict the expansion of the growing gut tube[68]. Circumferential constraint first leads to the formation of longitudinal ridges inside the gut. These ridges further buckle as longitudinal muscles develop that constrain the epithelium lengthwise and zigzag ridges form. Non-uniform proliferation then drives the formation of individual villi from the zigzag ridges.

In parallel, the gut tube as a whole buckles and forms highly stereotyped loops. The gut tube is attached to the dorsal mesentery along its length, which acts as an anchor for the gut in the abdomen (Figure 3E). Detailed measurements of the embryonic chicken gut revealed that the gut tube grows about three times as fast as the mesentery[69]. The mesentery thus acts as a physical constraint and induces buckling of the gut tube. The shape of the loops that form can be predicted based on the geometry and elastic modulus of the gut and the mesentery. Bone morphogenetic protein 2 (Bmp2) signaling suppresses the growth of the mesentery and thereby controls the length difference between the mesentery and the gut tube[70]. Blocking Bmp2 signaling increases mesenteric growth and generates larger loops. Conversely, overactivating Bmp2 signaling decreases mesenteric growth and generates small, tight loops. Thus, balanced — but differential — growth rates of the neighboring tissues lead to stereotyped buckling, ensuring that the gut fits within the abdomen.

Branching morphogenesis

Organs such as the lung, mammary gland, and kidney maximize their epithelial surface area within a confined volume by multiple rounds of branching that result in a tree-like structure. Branching is conceptually similar to the tissue invagination discussed above and can be viewed as a special case in which invaginations occur from an already existing epithelial tube. Consequently, similar epithelial packing motifs, such as apical constriction and buckling (Figure 3A), are observed during branch initiation. These new branches then lengthen by using tissue elongation motifs, such as cell rearrangements and oriented cell division (Figure 2A). Thus, a combination of tissue invagination and tissue elongation motifs can generate tissues with complex shapes such as branched organs.

Smooth muscle shapes the buckling airway epithelium into branches in the mouse lung

The mammalian lung forms by a series of domain branches and bifurcation events[71]. Domain branches form along the side of an existing branch, whereas bifurcations split the tip of a branch into two daughter branches. Both types of branches are influenced by smooth muscle wrapping around the airway epithelium[72,73]. Due to the luminal pressure inside the developing lung, regions that are not covered by smooth muscle bulge outwards into the surrounding mesenchyme at stereotyped locations to initiate daughter branches (Figure 4A). Increasing smooth muscle wrapping via pharmacological means reduces the frequency of branch initiation. Conversely, decreasing smooth muscle wrapping by pharmacological or genetic approaches results in uncontrolled buckling of the epithelium. Similar buckling can be observed in mesenchyme-free cultures of the airway epithelium, which lack smooth muscle entirely[74] (Figure 4B). Taken together, these observations demonstrate that smooth muscle wrapping constrains buckling to defined locations, leading to stereotyped formation of branches in the mammalian lung.

Apical constriction drives branching in the avian lung

Similar to the mammalian lung, the main branches of the avian lung form by domain branching. However, smooth muscle does not appear until later stages of avian lung development. Thus, smooth muscle wrapping is not required for branch initiation in the avian lung. Instead, branch initiation is achieved by

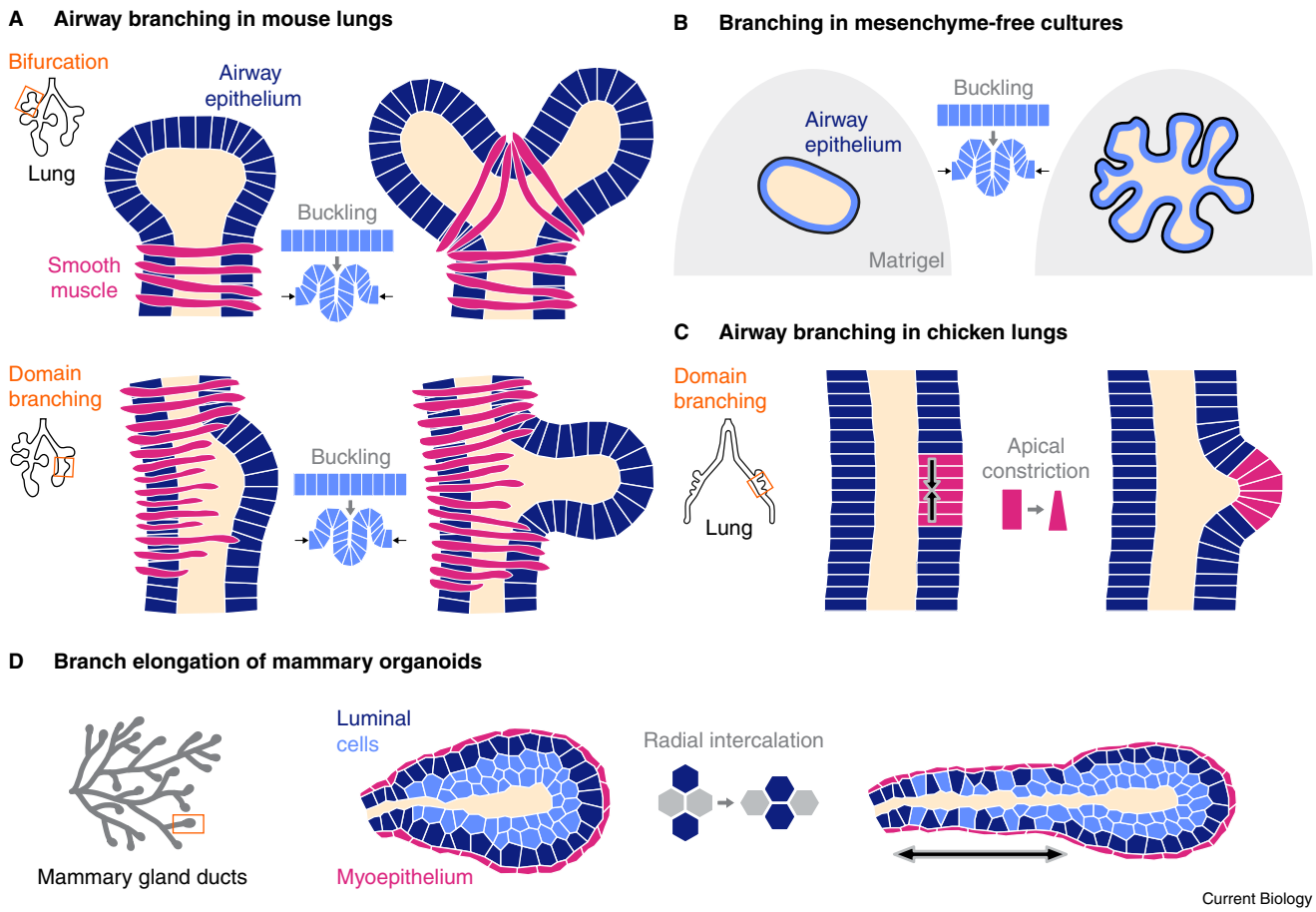

Figure 4. Mechanisms used to achieve branching of epithelial tissues.
(A–D) Examples of branching morphogenesis. Icons of the cellular motifs introduced in Figures 2A and 3A indicate how epithelial branching is achieved at the respective developmental steps. (A) Airway branching in mouse lungs. Schematic of airway bifurcation and domain branching shaped by smooth muscle wrapping in the embryonic mouse lung. (B) Branching in mesenchyme-free cultures. Buckling of the airway epithelium can be studied in 3D culture in Matrigel after removal of the surrounding mesenchyme. (C) Airway branching in the embryonic chicken lung is driven by apical constriction of the epithelial cells. Note the absence of smooth muscle at this stage of development. (D) Branch elongation of mammary organoids. Radial intercalation of luminal cells drives the elongation of mammary organoids in the presence of circumferential tension exerted by the surrounding myoepithelium.

local apical constriction, which results in the formation of an epithelial bud[75,76] (Figure 4C). If cell proliferation is blocked pharmacologically, the epithelium still buds; therefore, local proliferation is not required for branch initiation[75]. Computational modeling of apical constriction can mimic the process of branch initiation but is not sufficient to explain branch elongation. More recent work revealed that degradation of the basement membrane at branch tips allows the branches to elongate while deforming adjacent mesenchymal cells[77]. Thus, apical constriction drives branch initiation in the avian lung, and branch elongation is accommodated by basement membrane degradation and fluidity of the mesenchyme.

Radial cell intercalation elongates branches in mammary organoids

The mammary gland consists of tree-like epithelial ducts embedded in the mammary fat pad. The mechanisms of bifurcation and side branching are unknown. Since the fat pad is large and opaque, live imaging is very challenging. Therefore, mammary organoids embedded in 3D gels of ECM have been used to study branching morphogenesis and branch elongation[78]. Similar to mesenchyme-free lung epithelia, mammary organoids branch as they grow in culture. The tips of these branches consist of multiple layers of cells: inner cells are surrounded by an outer layer of luminal cells, which are surrounded by myoepithelial cells (Figure 4D). The inner cells radially intercalate into the outer layer of luminal cells and thereby elongate the branches[79]. Modeling of this process showed that radial intercalation only leads to elongation in the presence of a circumferential stress (hoop stress) generated by the surrounding myoepithelial cells. *In vivo*, mammary branches are surrounded by adipocytes, and branches need to squeeze in between these adipocytes to elongate. How the presence of adipocytes affects branching of the mammary ducts remains to be uncovered.

How can we use tissue engineering to recreate cell packing to generate functional tissues?

The previous sections were focused on understanding how epithelial cell packing motifs contribute to morphogenesis of different organs. In this section, we analyze how cell packing is controlled in tissue-engineering applications to create organs[80].

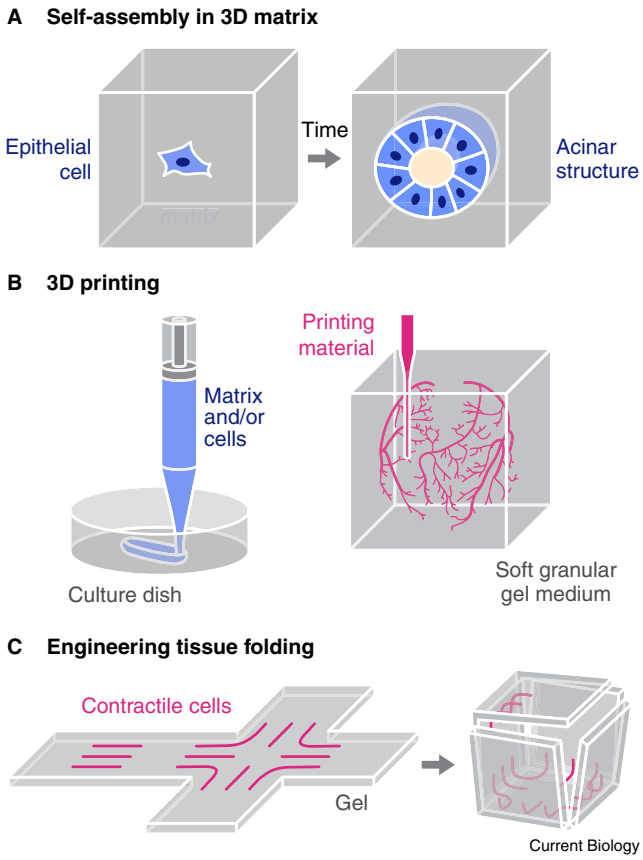

Figure 5. Approaches to recreate epithelial cell packing in 3D organotypic culture models.
(A) Epithelial cells, such as MCF10A mammary epithelial cells, spontaneously self-assemble into spherical acini with a hollow lumen when cultured in 3D. (B) 3D printing is a powerful tool to create matrices such as collagen with aligned fibers and to place cells into a matrix at predefined locations. Subsequent culture allows the cells to interact with each other and generate organ-like 3D structures. (C) Tissue folding driven by contractile cell types placed in strategic patterns on a flexible substratum. Here, a schematic of a cube formed in 3D from a planar network is shown[89].

A common strategy to create tissues is to take advantage of the ability of cells to self-assemble. Single epithelial cells placed in a 3D matrix like collagen or Matrigel often form acinar structures with a hollow lumen as they proliferate[81,82] (Figure 5A). To create shapes other than spheroids, cavities with defined geometries can be micromolded into the matrix; cells cultured in these cavities form tissues that conform to the surrounding geometry, for example elongated tubules[83,84]. Furthermore, buckled epithelia can be generated by growing epithelial cells inside a stiff alginate shell[85].

To control cell packing more directly, 3D-printing methods are being adapted. Hydrogels or cell–hydrogel mixtures can be 3D-printed onto a culture dish (Figure 5B). Similar to a conventional 3D printer, the printing path determines the shape of the structure and multiple layers of printing can be used to create a 3D structure[86]. Alternatively, a soft granular gel medium can be used as a matrix into which cells are placed anywhere in 3D using a needle that moves through the gel (Figure 5B). The granular gel transiently fluidizes around the needle and quickly resolidifies to support the printed structure[87,88]. Therefore, delicate structures like a branched network can be created.

3D printing excels at placing cells in a defined position; however, a key feature of a functional tissue is cell–cell interaction. Simply placing cells next to each other is not always sufficient to induce these cells to interact in the absence of developmental context. An exciting avenue to simulate morphogenesis and provide cells with a developmental context is engineered tissue folding. Rather than creating the final 3D structure, a 2D blueprint can be generated that then folds into the desired 3D shape. For example, contractile cells placed at strategic positions on a cube net made of gel can fold the planar gel into a 3D cube[89] (Figure 5C).

Conclusion and perspectives

To shape organs during morphogenesis, epithelial tissues expand, shrink, elongate, fold, invaginate, and branch. Here, we highlight cellular motifs that result in these shape changes. This collection of motifs can be viewed as the toolbox of morphogenesis. Just as different tools like a handsaw or a jigsaw can be used to cut wood into a desired shape, different cellular motifs like rearrangements or oriented cell division can lead to elongation of an epithelial tissue. During morphogenesis, these motifs are often combined, permitting a tissue like the *Drosophila* wing to elongate in response to cell-shape changes, rearrangements, and oriented cell divisions[5,41–45].

In addition, changes in shape can result from forces exerted by neighboring tissues. For example, the hinge area of the wing compacts and pulls on the wing blade[43,44], and the dorsal mesentery exerts compressive force on the gut tube, which then buckles as a result[69]. Neighboring tissues also need to adapt to accommodate shape changes; for example, the dorsal tissue of the *Drosophila* embryo needs to soften and expand to allow the mesoderm to fold and invaginate on the ventral side[59]. The combination of different motifs generates the diverse shapes of tissues, including those with high complexity, like the branched network of airways in the mammalian lung[71–73].

Tissue-engineering approaches like 3D bioprinting have been exploited in recent years with the aim of recreating organs in culture[86–88]. These approaches take advantage of the capacity of cells to self-assemble in microenvironments that mimic their native surroundings. Many current tissue-engineering strategies are designed to position cells at their final location in a 3D construct, hoping that they will interact with their neighbors to form an intact tissue. We propose that future tissue-engineering strategies should consider the mechanisms that are used by developing organs. Recapitulating the stages of morphogenesis of the native tissue might provide the cells with the history that is required for forming functional interactions. Future studies investigating how epithelial tissues are shaped by dynamic changes in cell packing will thus both contribute to our understanding of morphogenesis and inform endeavors in tissue engineering.

ACKNOWLEDGEMENTS

Work from the authors' group was supported in part by grants from the National Institutes of Health (HL120142, HD079030, CA214292) and a Faculty Scholars Award from the Howard Hughes Medical Institute. S.B.L. was

supported in part by the Deutsche Forschungsgemeinschaft (DFG, German Research Foundation; 459686752). The authors thank Payam Farahani for providing the microscopy data used for generating Figure 1E.

DECLARATION OF INTERESTS

The authors declare no competing interests.

REFERENCES

1. Gehr, P., Bachofen, M., and Weibel, E.R. (1978). The normal human lung: ultrastructure and morphometric estimation of diffusion capacity. Respir. Physiol. *32*, 121–140.

2. Venkatachalam, M.A., and Rennke, H.G. (1978). The structural and molecular basis of glomerular filtration. Circ. Res. *43*, 337–347.

3. Ferraro, F., Celso, C.L., and Scadden, D. (2010). Adult stem cells and their niches. Adv. Exp. Med. Biol. *695*, 155–168.

4. Guirao, B., Rigaud, S.U., Bosveld, F., Bailles, A., López-Gay, J., Ishihara, S., Sugimura, K., Graner, F., and Bellaïche, Y. (2015). Unified quantitative characterization of epithelial tissue development. eLife *4*, e08519.

5. Diaz-de-la-Loza, M.C., and Thompson, B.J. (2017). Forces shaping the Drosophila wing. Mech. Dev. *144*, 23–32.

6. Gómez-Gálvez, P., Vicente-Munuera, P., Tagua, A., Forja, C., Castro, A.M., Letrán, M., Valencia-Expósito, A., Grima, C., Bermúdez-Gallardo, M., Serrano-Pérez-Higueras, O., *et al*. (2018). Scutoids are a geometrical solution to three-dimensional packing of epithelia. Nat. Commun. *9*, 2960.

7. Ramanathan, S.P., Krajnc, M., and Gibson, M.C. (2019). Cell-size pleomorphism drives aberrant clone dispersal in proliferating epithelia. Dev. Cell *51*, 49–61.e4.

8. Bosveld, F., Wang, Z., and Bellaïche, Y. (2018). Tricellular junctions: a hot corner of epithelial biology. Curr. Opin. Cell Biol. *54*, 80–88.

9. Byri, S., Misra, T., Syed, Z.A., Bätz, T., Shah, J., Boril, L., Glashauser, J., Aegerter-Wilmsen, T., Matzat, T., Moussian, B., *et al*. (2015). The triple-repeat protein Anakonda controls epithelial tricellular junction formation in Drosophila. Dev. Cell *33*, 535–548.

10. Isasti-Sanchez, J., Münz-Zeise, F., Lancino, M., and Luschnig, S. (2021). Transient opening of tricellular vertices controls paracellular transport through the follicle epithelium during Drosophila oogenesis. Dev. Cell *56*, 1083–1099.e5.

11. Yu, H.H., and Zallen, J.A. (2020). Abl and Canoe/Afadin mediate mechanotransduction at tricellular junctions. Science *370*, eaba5528.

12. Bosveld, F., Markova, O., Guirao, B., Martin, C., Wang, Z., Pierre, A., Balakireva, M., Gaugue, I., Ainslie, A., Christophorou, N., *et al*. (2016). Epithelial tricellular junctions act as interphase cell shape sensors to orient mitosis. Nature *530*, 495–498.

13. Sanchez-Corrales, Y.E., Blanchard, G.B., and Roper, K. (2018). Radially patterned cell behaviours during tube budding from an epithelium. eLife *7*, e35717.

14. Sánchez-Gutiérrez, D., Sáez, A., Gómez-Gálvez, P., Paradas, C., and Escudero, L.M. (2017). Rules of tissue packing involving different cell types: human muscle organization. Sci. Rep. *7*, 40444.

15. Thompson, D.A.W. (1917). On Growth and Form (Cambridge: Cambridge University Press).

16. Graner, F., and Riveline, D. (2017). 'The Forms of Tissues, or Cell-aggregates': D'Arcy Thompson's influence and its limits. Development *144*, 4226–4237.

17. Lecuit, T., and Lenne, P.-F. (2007). Cell surface mechanics and the control of cell shape, tissue patterns and morphogenesis. Nat. Rev. Mol. Cell Biol. *8*, 633–644.

18. Bi, D., Lopez, J.H., Schwarz, J.M., and Manning, M.L. (2015). A density-independent rigidity transition in biological tissues. Nat. Phys. *11*, 1074–1079.

19. Wang, X., Merkel, M., Sutter, L.B., Erdemci-Tandogan, G., Manning, M.L., and Kasza, K.E. (2020). Anisotropy links cell shapes to tissue flow during convergent extension. Proc. Natl. Acad. Sci. USA *117*, 13541–13551.

20. Simone, R.P., and Dinardo, S. (2010). Actomyosin contractility and Discs large contribute to junctional conversion in guiding cell alignment within the Drosophila embryonic epithelium. Development *137*, 1385–1394.

21. Chiou, K.K., Hufnagel, L., and Shraiman, B.I. (2012). Mechanical stress inference for two dimensional cell arrays. PLoS Comput. Biol. *8*, e1002512.

22. Ishihara, S., and Sugimura, K. (2012). Bayesian inference of force dynamics during morphogenesis. J. Theor. Biol. *313*, 201–211.

23. Ishihara, S., Sugimura, K., Cox, S.J., Bonnet, I., Bellaïche, Y., and Graner, F. (2013). Comparative study of non-invasive force and stress inference methods in tissue. Eur. Phys. J. E *36*, 9859.

24. Brodland, G.W., Veldhuis, J.H., Kim, S., Perrone, M., Mashburn, D., and Hutson, M.S. (2014). CellFIT: a cellular force-inference toolkit using curvilinear cell boundaries. PLoS One *9*, e99116.

25. Aigouy, B., Umetsu, D., and Eaton, S. (2016). Segmentation and quantitative analysis of epithelial tissues. In Drosophila: Methods and Protocols, C. Dahmann, ed. (New York, NY: Springer New York), pp. 227–239.

26. Tinevez, J.-Y., Perry, N., Schindelin, J., Hoopes, G.M., Reynolds, G.D., Laplantine, E., Bednarek, S.Y., Shorte, S.L., and Eliceiri, K.W. (2017). TrackMate: An open and extensible platform for single-particle tracking. Methods *115*, 80–90.

27. McQuin, C., Goodman, A., Chernyshev, V., Kamentsky, L., Cimini, B.A., Karhohs, K.W., Doan, M., Ding, L., Rafelski, S.M., Thirstrup, D., *et al*. (2018). CellProfiler 3.0: Next-generation image processing for biology. PLoS Biol. *16*, e2005970.

28. Etournay, R., Merkel, M., Popović, M., Brandl, H., Dye, N.A., Aigouy, B., Salbreux, G., Eaton, S., and Jülicher, F. (2016). TissueMiner: a multiscale analysis toolkit to quantify how cellular processes create tissue dynamics. eLife *5*, e14334.

29. Merkel, M., Etournay, R., Popović, M., Salbreux, G., Eaton, S., and Jülicher, F. (2017). Triangles bridge the scales: Quantifying cellular contributions to tissue deformation. Phys. Rev. E *95*, 032401.

30. Clarke, D.N., and Martin, A.C. (2021). Actin-based force generation and cell adhesion in tissue morphogenesis. Curr. Biol. *31*, R667–R680.

31. Wang, M.F.Z., Hunter, M., Wang, G., Mcfaul, C., Yip, C.M., and Fernandez-Gonzalez, R. (2017). Automated cell tracking identifies mechanically-oriented cell divisions during Drosophila axis elongation. Development *144*, 1350–1361.

32. Finegan, T.M., Na, D., Cammarota, C., Skeeters, A.V., Nádasi, T.J., Dawney, N.S., Fletcher, A.G., Oakes, P.W., and Bergstralh, D.T. (2019). Tissue tension and not interphase cell shape determines cell division orientation in the Drosophila follicular epithelium. EMBO J. *38*, e100072.

33. Scarpa, E., Finet, C., Blanchard, G.B., and Sanson, B. (2018). Actomyosin-driven tension at compartmental boundaries orients cell division independently of cell geometry in vivo. Dev. Cell *47*, 727–740.e6.

34. Gu, Y., and Rosenblatt, J. (2012). New emerging roles for epithelial cell extrusion. Curr. Opin. Cell Biol. *24*, 865–870.

35. Toyama, Y., Peralta, X.G., Wells, A.R., Kiehart, D.P., and Edwards, G.S. (2008). Apoptotic force and tissue dynamics during Drosophila embryogenesis. Science *321*, 1683–1686.

36. Sadati, M., Taheri Qazvini, N., Krishnan, R., Park, C.Y., and Fredberg, J.J. (2013). Collective migration and cell jamming. Differentiation *86*, 121–125.

37. Bi, D., Yang, X., Marchetti, M.C., and Manning, M.L. (2016). Motility-driven glass and jamming transitions in biological tissues. Phys. Rev. X *6*, 021011.

38. Jain, A., Ulman, V., Mukherjee, A., Prakash, M., Cuenca, M.B., Pimpale, L.G., Münster, S., Haase, R., Panfilio, K.A., Jug, F., *et al*. (2020). Regionalized tissue fluidization is required for epithelial gap closure during insect gastrulation. Nat. Commun. *11*, 5604.

39. Lawton, A.K., Nandi, A., Stulberg, M.J., Dray, N., Sneddon, M.W., Pontius, W., Emonet, T., and Holley, S.A. (2013). Regulated tissue fluidity steers zebrafish body elongation. Development *140*, 573–582.

40. Mongera, A., Rowghanian, P., Gustafson, H.J., Shelton, E., Kealhofer, D.A., Carn, E.K., Serwane, F., Lucio, A.A., Giammona, J., and Campàs, O. (2018). A fluid-to-solid jamming transition underlies vertebrate body axis elongation. Nature *561*, 401–405.

41. Dye, N.A., Popović, M., Spannl, S., Etournay, R., Kainmüller, D., Ghosh, S., Myers, E.W., Jülicher, F., and Eaton, S. (2017). Cell dynamics underlying oriented growth of the Drosophila wing imaginal disc. Development *144*, 4406–4421.

42. Diaz-de-la-Loza, M.D., Ray, R.P., Ganguly, P.S., Alt, S., Davis, J.R., Hoppe, A., Tapon, N., Salbreux, G., and Thompson, B.J. (2018). Apical and basal matrix remodeling control epithelial morphogenesis. Dev. Cell *46*, 23–39.e5.

43. Ray, R.P., Matamoro-Vidal, A., Ribeiro, P.S., Tapon, N., Houle, D., Salazar-Ciudad, I., and Thompson, B.J. (2015). Patterned anchorage to the apical extracellular matrix defines tissue shape in the developing appendages of Drosophila. Dev. Cell *34*, 310–322.

44. Etournay, R., Popović, M., Merkel, M., Nandi, A., Blasse, C., Aigouy, B., Brandl, H., Myers, G., Salbreux, G., Jülicher, F., *et al*. (2015). Interplay of cell dynamics and epithelial tension during morphogenesis of the Drosophila pupal wing. eLife *4*, e07090.

45. Aigouy, B., Farhadifar, R., Staple, D.B., Sagner, A., Röper, J.-C., Jülicher, F., and Eaton, S. (2010). Cell flow reorients the axis of planar polarity in the wing epithelium of Drosophila. Cell *142*, 773–786.

46. Wyngaarden, L.A., Vogeli, K.M., Ciruna, B.G., Wells, M., Hadjantonakis, A.K., and Hopyan, S. (2010). Oriented cell motility and division underlie early limb bud morphogenesis. Development *137*, 2551–2558.

47. Boehm, B., Westerberg, H., Lesnicar-Pucko, G., Raja, S., Rautschka, M., Cotterell, J., Swoger, J., and Sharpe, J. (2010). The role of spatially controlled cell proliferation in limb bud morphogenesis. PLoS Biol. *8*, e1000420.

48. Suzuki, T., and Morishita, Y. (2017). A quantitative approach to understanding vertebrate limb morphogenesis at the macroscopic tissue level. Curr. Opin. Genet. Dev. *45*, 108–114.

49. Morishita, Y., Kuroiwa, A., and Suzuki, T. (2015). Quantitative analysis of tissue deformation dynamics reveals three characteristic growth modes and globally aligned anisotropic tissue deformation during chick limb development. Development *142*, 1672–1683.

50. Lau, K., Tao, H., Liu, H., Wen, J., Sturgeon, K., Sorfazlian, N., Lazic, S., Burrows, J.T.A., Wong, M.D., Li, D., *et al*. (2015). Anisotropic stress orients remodelling of mammalian limb bud ectoderm. Nat. Cell Biol. *17*, 569–579.

51. Box, K., Joyce, B.W., and Devenport, D. (2019). Epithelial geometry regulates spindle orientation and progenitor fate during formation of the mammalian epidermis. eLife *8*, e47102.

52. Arraf, A.A., Yelin, R., Reshef, I., Jadon, J., Abboud, M., Zaher, M., Schneider, J., Vladimirov, F.K., and Schultheiss, T.M. (2020). Hedgehog signaling regulates epithelial morphogenesis to position the ventral embryonic midline. Dev. Cell *53*, 589–602.e6.

53. Monier, B., Gettings, M., Gay, G., Mangeat, T., Schott, S., Guarner, A., and Suzanne, M. (2015). Apico-basal forces exerted by apoptotic cells drive epithelium folding. Nature *518*, 245–248.

54. Sweeton, D., Parks, S., Costa, M., and Wieschaus, E. (1991). Gastrulation in Drosophila: the formation of the ventral furrow and posterior midgut invaginations. Development *112*, 775–789.

55. Kam, Z., Minden, J.S., Agard, D.A., Sedat, J.W., and Leptin, M. (1991). Drosophila gastrulation: analysis of cell shape changes in living embryos by three-dimensional fluorescence microscopy. Development *112*, 365–370.

56. Leptin, M., and Grunewald, B. (1990). Cell shape changes during gastrulation in Drosophila. Development *110*, 73–84.

57. Martin, A.C. (2020). The physical mechanisms of Drosophila gastrulation: mesoderm and endoderm invagination. Genetics *214*, 543–560.

58. Denk-Lobnig, M., Totz, J.F., Heer, N.C., Dunkel, J., and Martin, A.C. (2021). Combinatorial patterns of graded RhoA activation and uniform F-actin depletion promote tissue curvature. Development *148*, dev199232.

59. Rauzi, M., Krzic, U., Saunders, T.E., Krajnc, M., Ziherl, P., Hufnagel, L., and Leptin, M. (2015). Embryo-scale tissue mechanics during Drosophila gastrulation movements. Nat. Commun. *6*, 8677.

60. Streichan, S.J., Lefebvre, M.F., Noll, N., Wieschaus, E.F., and Shraiman, B.I. (2018). Global morphogenetic flow is accurately predicted by the spatial distribution of myosin motors. eLife *7*, e27454.

61. Girdler, G.C., and Röper, K. (2014). Controlling cell shape changes during salivary gland tube formation in Drosophila. Semin. Cell Dev. Biol. *31*, 74–81.

62. Nelson, C.M. (2016). On buckling morphogenesis. J. Biomech. Eng. *138*, 021005.

63. Tozluoglu, M., Duda, M., Kirkland, N.J., Barrientos, R., Burden, J.J., Munoz, J.J., and Mao, Y. (2019). Planar differential growth rates initiate precise fold positions in complex epithelia. Dev. Cell *51*, 299–312.e4.

64. Nematbakhsh, A., Levis, M., Kumar, N., Chen, W., Zartman, J.J., and Alber, M. (2020). Epithelial organ shape is generated by patterned actomyosin contractility and maintained by the extracellular matrix. PLoS Comput. Biol. *16*, e1008105.

65. Badugu, A., and Käch, A. (2020). Independent apical and basal mechanical systems determine cell and tissue shape in the Drosophila wing disc. bioRxiv, https://doi.org/10.1101/2020.04.10.036152.

66. Huycke, T.R., and Tabin, C.J. (2018). Chick midgut morphogenesis. Int. J. Dev. Biol. *62*, 109–119.

67. Helander, H.F., and Fändriks, L. (2014). Surface area of the digestive tract – revisited. Scand. J. Gastroenterol. *49*, 681–689.

68. Shyer, A.E., Tallinen, T., Nerurkar, N.L., Wei, Z., Gil, E.S., Kaplan, D.L., Tabin, C.J., and Mahadevan, L. (2013). Villification: how the gut gets its villi. Science *342*, 212–218.

69. Savin, T., Kurpios, N.A., Shyer, A.E., Florescu, P., Liang, H., Mahadevan, L., and Tabin, C.J. (2011). On the growth and form of the gut. Nature *476*, 57–62.

70. Nerurkar, N.L., Mahadevan, L., and Tabin, C.J. (2017). BMP signaling controls buckling forces to modulate looping morphogenesis of the gut. Proc. Natl. Acad. Sci. USA *114*, 2277–2282.

71. Metzger, R.J., Klein, O.D., Martin, G.R., and Krasnow, M.A. (2008). The branching programme of mouse lung development. Nature *453*, 745–750.

72. Kim, H.Y., Pang, M.F., Varner, V.D., Kojima, L., Miller, E., Radisky, D.C., and Nelson, C.M. (2015). Localized smooth muscle differentiation is essential for epithelial bifurcation during branching morphogenesis of the mammalian lung. Dev. Cell *34*, 719–726.

73. Goodwin, K., Mao, S., Guyomar, T., Miller, E., Radisky, D.C., Kosmrlj, A., and Nelson, C.M. (2019). Smooth muscle differentiation shapes domain branches during mouse lung development. Development *146*, dev181172.

74. Varner, V.D., Gleghorn, J.P., Miller, E., Radisky, D.C., and Nelson, C.M. (2015). Mechanically patterning the embryonic airway epithelium. Proc. Natl. Acad. Sci. USA *112*, 9230–9235.

75. Kim, H.Y., Varner, V.D., and Nelson, C.M. (2013). Apical constriction initiates new bud formation during monopodial branching of the embryonic chicken lung. Development *140*, 3146–3155.

76. Tzou, D., Spurlin 3rd, J.W., Pavlovich, A.L., Stewart, C.R., Gleghorn, J.P., and Nelson, C.M. (2016). Morphogenesis and morphometric scaling of lung airway development follows phylogeny in chicken, quail, and duck embryos. EvoDevo *7*, 12.

77. Spurlin, J.W., Siedlik, M.J., Nerger, B.A., Pang, M.-F., Jayaraman, S., Zhang, R., and Nelson, C.M. (2019). Mesenchymal proteases and tissue fluidity remodel the extracellular matrix during airway epithelial branching in the embryonic avian lung. Development *146*, dev175257.

78. Srivastava, V., Huycke, T.R., Phong, K.T., and Gartner, Z.J. (2020). Organoid models for mammary gland dynamics and breast cancer. Curr. Opin. Cell Biol. *66*, 51–58.

79. Neumann, N.M., Perrone, M.C., Veldhuis, J.H., Huebner, R.J., Zhan, H., Devreotes, P.N., Brodland, G.W., and Ewald, A.J. (2018). Coordination of receptor tyrosine kinase signaling and interfacial tension dynamics drives radial intercalation and tube elongation. Dev. Cell *45*, 67–82.e6.

80. Guven, S., Chen, P., Inci, F., Tasoglu, S., Erkmen, B., and Demirci, U. (2015). Multiscale assembly for tissue engineering and regenerative medicine. Trends Biotechnol. *33*, 269–279.

81. Debnath, J., Muthuswamy, S.K., and Brugge, J.S. (2003). Morphogenesis and oncogenesis of MCF-10A mammary epithelial acini grown in three-dimensional basement membrane cultures. Methods *30*, 256–268.

82. Petersen, O.W., Ronnov-Jessen, L., Howlett, A.R., and Bissell, M.J. (1992). Interaction with basement membrane serves to rapidly distinguish growth and differentiation pattern of normal and malignant human breast epithelial cells. Proc. Natl. Acad. Sci. USA *89*, 9064–9068.

83. Piotrowski-Daspit, A.S., and Nelson, C.M. (2016). Engineering three-dimensional epithelial tissues embedded within extracellular matrix. J. Vis. Exp. *10*, 54283.

84. Nelson, C.M., Inman, J.L., and Bissell, M.J. (2008). Three-dimensional lithographically defined organotypic tissue arrays for quantitative analysis of morphogenesis and neoplastic progression. Nat. Protoc. *3*, 674–678.

85. Trushko, A., Di Meglio, I., Merzouki, A., Blanch-Mercader, C., Abuhattum, S., Guck, J., Alessandri, K., Nassoy, P., Kruse, K., Chopard, B., *et al*. (2020). Buckling of an epithelium growing under spherical confinement. Dev. Cell *54*, 655–668.e6.

86. Nerger, B.A., and Nelson, C.M. (2020). Bioprinting cell-laden hydrogels for studies of epithelial tissue morphogenesis. In Tissue Morphogenesis, Methods in Molecular Biology series, C.M. Nelson, ed. (Springer Nature), in press.

87. Morley, C.D., Ellison, S.T., Bhattacharjee, T., O'Bryan, C.S., Zhang, Y., Smith, K.F., Kabb, C.P., Sebastian, M., Moore, G.L., Schulze, K.D., *et al*. (2019). Quantitative characterization of 3D bioprinted structural elements under cell generated forces. Nat. Commun. *10*, 3029.

88. Bhattacharjee, T., Zehnder, S.M., Rowe, K.G., Jain, S., Nixon, R.M., Sawyer, W.G., and Angelini, T.E. (2015). Writing in the granular gel medium. Sci. Adv. *1*, e1500655.

89. Hughes, A.J., Miyazaki, H., Coyle, M.C., Zhang, J., Laurie, M.T., Chu, D., Vavrušová, Z., Schneider, R.A., Klein, O.D., and Gartner, Z.J. (2018). Engineered tissue folding by mechanical compaction of the mesenchyme. Dev. Cell *44*, 165–178.e6.